J. Foth, R. Marissen,† K.-H. Trautmann,† and H. Nowack†*

Short Crack Phenomena in a High Strength Aluminium Alloy and Some Analytical Tools for Their Prediction

REFERENCE Foth, J., Marissen, R., Trautmann, K.-H., and Nowack, H., **Short Crack Phenomena in a High Strength Aluminium Alloy and Some Analytical Tools for Their Prediction**, *The Behaviour of Short Fatigue Cracks*, EGF Pub. 1 (Edited by K. J. Miller and E. R. de los Rios) 1986, Mechanical Engineering Publications, London, pp. 353–368.

ABSTRACT Short cracks show in many aspects a different behaviour to that predicted on the basis of long crack properties. This is especially true for microstructurally short cracks. As the cracks become longer they may grow through a regime denoted as mechanically short cracks. The present investigation presents results of the mechanically short crack regime in unnotched and notched Al 2024-T3 specimens and proposes a rational fracture-mechanics based approach for semielliptical surface cracks within an arbitrary stress field.

For a moderate plastic environment for short cracks in a notch field the notch root stress and strain ratios attain a special significance. Calculations based on the stress ratio, R_σ, described the lower bound of the short crack data. Predictions based on the strain ratio were more conservative.

Microstructurally short cracks showed a behaviour which could not be covered by the described crack growth evaluation method.

Nomenclature

a	Crack depth
c	Crack length on the notch surface
f	Notch depth
da/dN	Crack propagation rate
K	Stress intensity factor
ΔK	Cyclic stress intensity factor
K_{CC}	Stress intensity factor of an embedded circular crack in a stress field without a gradient
K_{EC}	Stress intensity for a semi-elliptical crack in a specimen without a notch
K_{NCC}	Stress intensity factor of an embedded circular crack in a stress field with a stress gradient
K_{NEC}	Stress intensity factor for a semi-elliptical crack at a notch
K_t	Stress concentration factor
K_x	Stress intensity due to an incremental stress $\sigma(x)$
l	Crack length from the notch root

* *Presently* Project Engineer, Fatigue and Fracture Mechanics, IABG, D-8012 Ottobrunn, FRG; *Formerly* Researcher, Fatigue Branch, DFVLR, D-5000 Cologne 90, FRG.
† Fatigue Branch, DFVLR, D-5000 Cologne 90, FRG.

N	Cycle number
r, φ	Polar coordinates
R	Stress ratio
R_ε	Strain ratio at the notch root
R_σ	Stress ratio at the notch root
S	Nominal stress
ε	Local strain
ε_{max}	Maximum local strain
ε_{min}	Minimum local strain
σ	Local stress
$\sigma(x) \cdot dx$	Wedge force at location x
σ_{max}	Maximum local stress
σ_{min}	Minimum local stress
ρ	Notch radius

Introduction

Short crack investigations have become a major subject of research work during the past 8–10 years. Several general trends of short crack behaviour have been observed. A survey is given in Fig. 1 (**1**). A classification of the short crack regime may be performed by a subdivision into two characteristic areas. At the beginning the size of the cracks correlates to microstructural features (such as grain size, length of slip bands, etc.). These cracks are denoted as microstructurally short cracks (see Fig. 1). As the cracks grow larger and reach higher da/dN vs ΔK values the microstructural influences become less significant and the mechanical environment of the cracks becomes more important. Cracks of the later category are denoted as mechanically short cracks (**2**).

When considering short cracks, for example in engineering design, analytical predictions have to be available. Based on the results of experimental investigations the present paper outlines some analytical tools for the representation and prediction of short crack behaviour.

Experimental investigations

In some previous publications (**3**)–(**5**) the results of an extensive experimental investigation of crack initiation and propagation behaviour of Al 2024-T3 specimens were given. Experimental details and the special mapping procedure which had been applied for the registration and reconstruction of the crack initiation, short crack and macro-crack behaviour were also described in the referenced publications. An overview of the results is given in Figs 2–5.

Figure 2 shows the specimen types. Unnotched and notched specimens were considered. In Fig. 3 the crack propagation behaviour and the microstructural features are presented as observed at the notch root of the $K_t = 3.3$ specimen (compare Fig. 2). The cracks always initiated at hard intermetallic inclusions

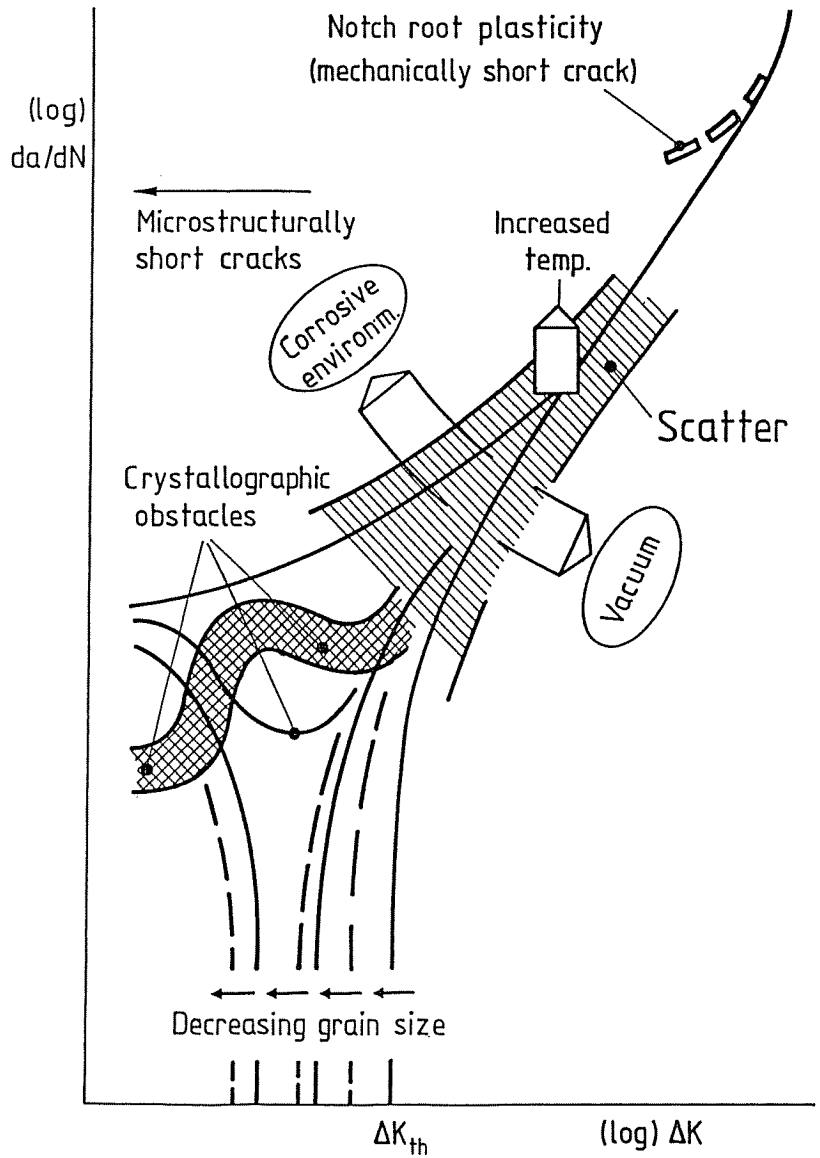

Fig 1 Characteristics of short cracks and transition to long crack behaviour

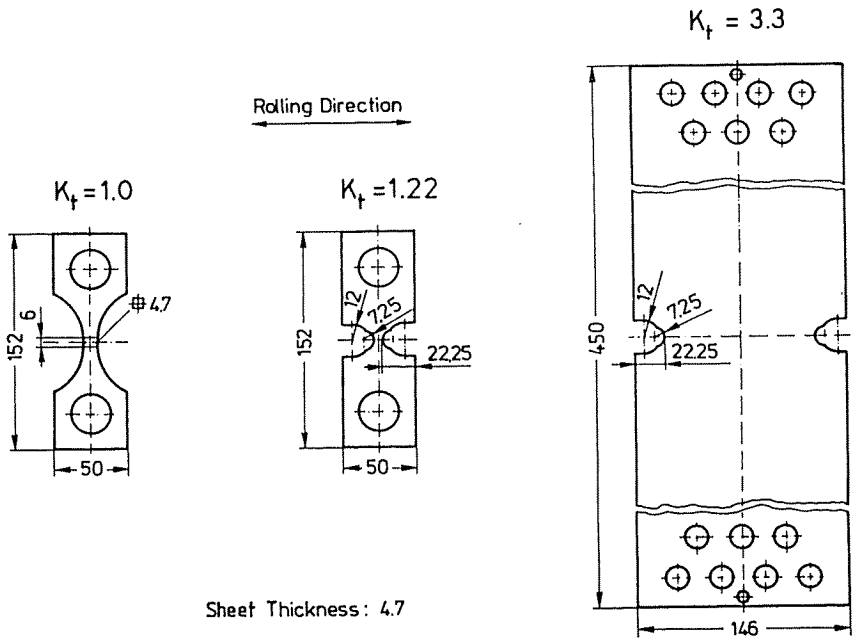

Fig 2 Specimens for the experimental investigations (dimensions in mm)

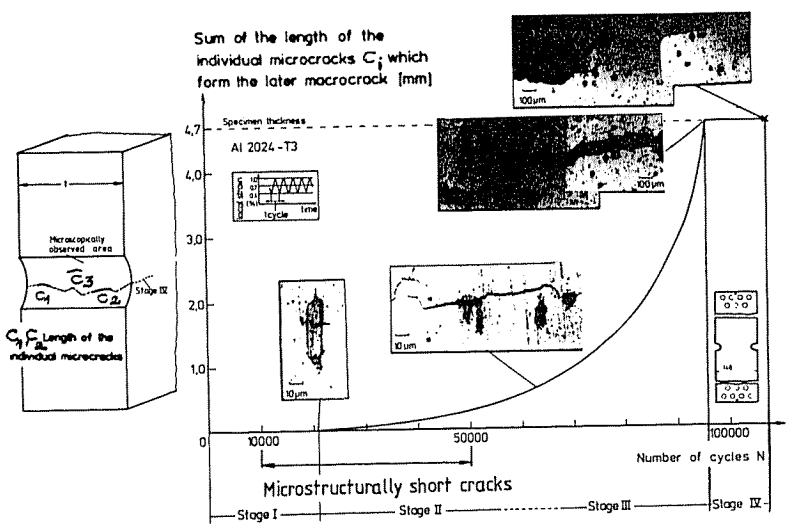

Fig 3 Stages of crack initiation and crack propagation at notched specimens, and the microstructurally short crack regime

for this material, and the period for cracks to attain a size at the notch surface of 50–100 μm is marked as stage I in the figure. For the loading level applied in the study cracks initiated at more than one location in the notch. The cracks grew at first independently of each other (stage II in Fig. 3), and some of them started to coalesce after some while to form the later macro-crack (stage III in Fig. 3). The macro-crack stage, when cracks become visible at the side surface of the notched specimen, is denoted as stage IV (not that on the ordinate of Fig. 3 the sum of the lengths only of those cracks which later formed the macro-crack is considered). Specially indicated in Fig. 3 is that range of lifetime where microstructurally short cracks are present.

Figure 4 shows the corresponding crack propagation behaviour of all three types of specimens used in this study. It can be clearly seen that the initiation of short cracks occurred at a similar number of cycles, but that this equivalence disappeared as the cracks grew larger. In the unnotched specimens the cracks rapidly increased in size, whereas for the notched specimens the cracks grew more slowly (due to the stress gradient behind the notch).

It has to be pointed out that the trends in Fig. 4 are subject to a very large scatter in experimental data. In order to visualize the scatter the test data for the notched specimen with $K_t = 3.3$ are given in Fig. 5 in the form of a da/dN vs crack length plot. It can be seen that the scatter band is very large at the beginning of growth, decreases in width as the cracks become larger, and develops into the growth direction as observed for long cracks as the crack length increases.

In the following a fracture-mechanics based interpretation of the crack propagation behaviour will be performed.

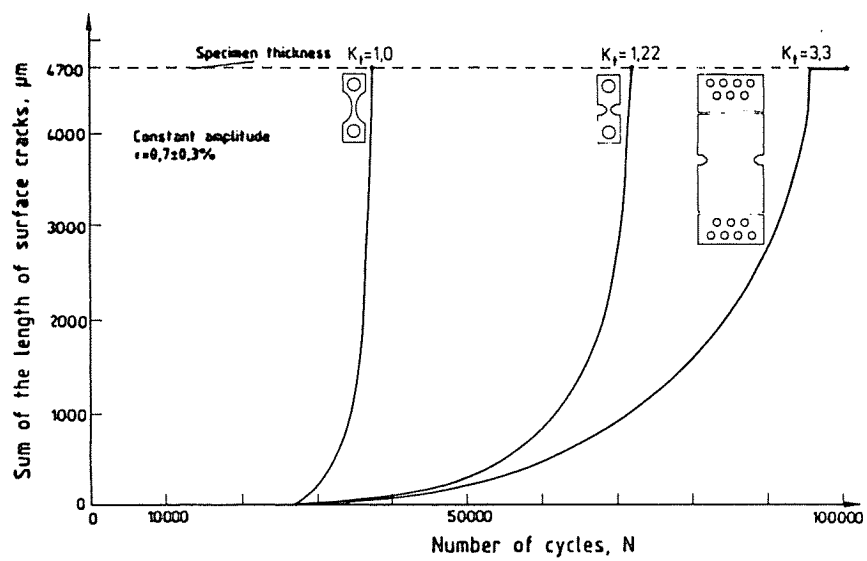

Fig 4 Crack initiation and propagation behaviour for the specimens shown in Fig. 2

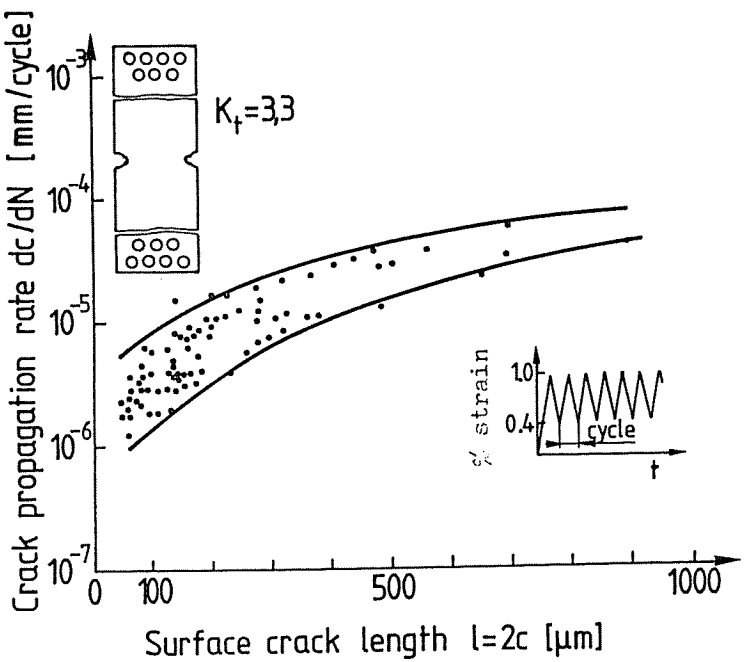

Fig 5 Scatter band of the crack propagation data as observed on the notch surface of $K_t = 3.3$ specimens

Evaluation of stress intensity factors

For a fracture mechanics based description of the propagation behaviour of short cracks, which are usually half or quarter elliptical, suitable stress intensity factors have to be available. For unnotched configurations such stress intensity factors have already been derived (**6**). In the case of notched specimens, solutions are available from the literature mainly for two-dimensional (through-thickness) problems (**7**)(**8**). Three-dimensional problems have also been considered by systematic finite element analyses and solutions are given either in the form of tabular solutions or as analytical expressions which are fitted to the tabular solutions (**9**). So far only cracks at unnotched specimens and at specimens with circular notches have been treated. In the following a procedure will be derived which may be applied to cases which are not covered by the present literature.

Basically, stress intensity factors for cracks at notches depend on the notch stress field (without a crack) and the crack length. The notch stress field is described by ρ, the notch root radius, by f, the notch depth, and by the applied stresses, S. That means that, altogether, four variables become relevant for the stress intensity in a notch field (up to a maximum distance from the notch of

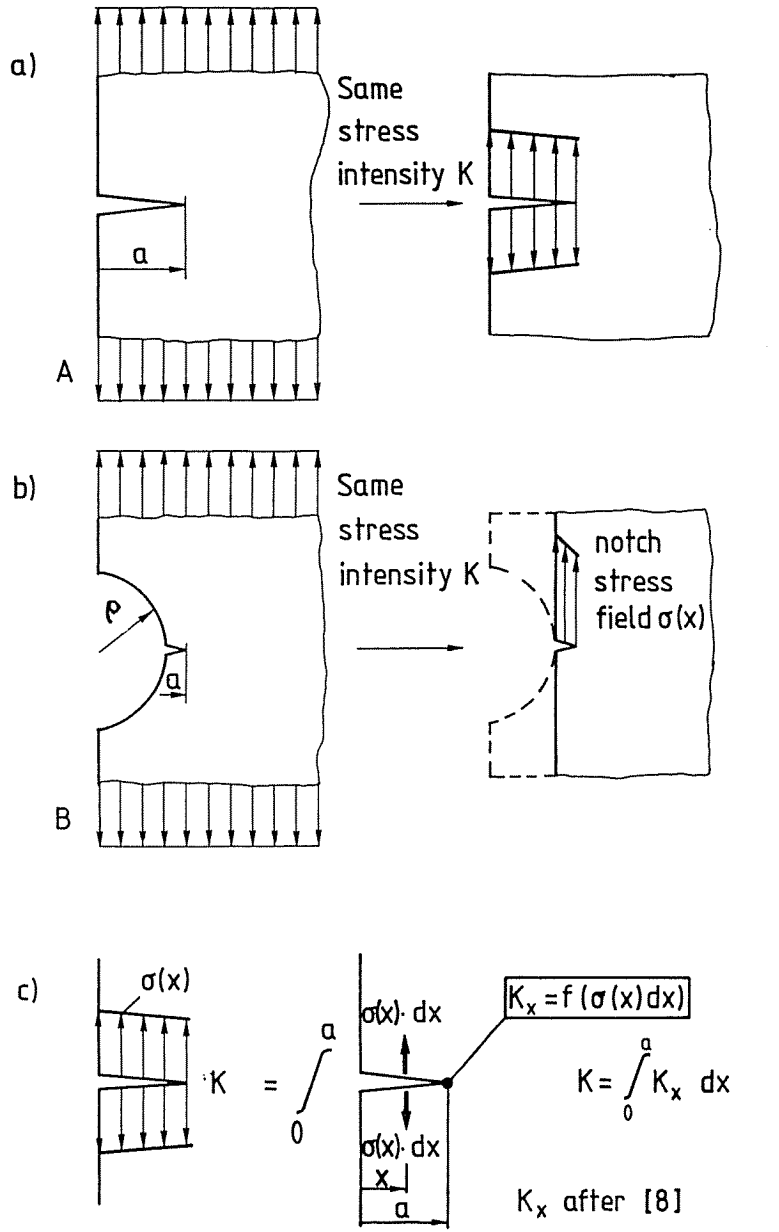

Fig 6 Evaluation of stress intensity factors in unnotched and notched configurations (two-dimensional case)

$\approx \rho/2$). Several authors have shown that stress intensity factors based on the described four variables yielded satisfactory results for two-dimensional cases (**10**)(**11**). However, practical solutions have not yet been established for the three-dimensional case; this is now proposed and the working principle is initially demonstrated, for the sake of simplicity, by a two-dimensional case.

Figure 6(a) shows how elementary fracture mechanics can be used to calculate the stress intensity factor for a semi-infinite plate containing an edge crack. Based on the wedge force model the remote stress has to be applied along the flanks of the crack. For a crack at a notch an analogous procedure is utilized (see Fig. 6(b)). This approximate solution remains satisfactory as long as the crack does not become too long as compared to the notch root radius, ρ. The calculation procedure for the stress intensity is given in Fig. 6(c). The notch stress field (without a crack) is split up into finite increments and individual wedge forces $\sigma(x) \cdot dx$ can be calculated. Each individual wedge force leads to a stress intensity factor $K_x = f\{\sigma(x) \cdot dx\}$ at the tip of the crack. The K_x values are then integrated over the entire crack length, a, to give the actual stress intensity factor at the crack tip. Values of K_x can be taken, for example, from stress intensity factor handbooks (**7**)(**8**).

The analogous procedure for the three-dimensional case is demonstrated in Fig. 7. Elementary solutions as mentioned in connection with Fig. 6(c) for the two-dimensional case are not yet available for three-dimensional problems. That is the reason why, for half or quarter elliptical crack shapes, a circular embedded crack in an infinite body is here taken as a basis. As mentioned before, the notch stress field (without a crack) has to be known and this has been calculated for the $K_t = 3.3$ specimen (which is the example here) by a finite element analysis (**2**)(**12**). The notch field is applied symmetrically to the circular embedded crack (see Fig. 7). Wedge forces are now calculated from the notch stress field for the whole area of the crack. Together with the stress intensity solution for the crack area (which is taken, for example, from a stress intensity handbook) individual stress intensity contributions at the crack tip can be evaluated. As demonstrated for the two-dimensional case in Fig. 6(c), an integration of the individual stress intensity contributions is performed (double integrals) and leads to the stress intensity factors, for example at A and B in Fig. 7 for the embedded crack, which are of special interest.

A similarity approach is now introduced for the evaluation of the stress intensity factor for a semi-elliptical surface crack at notches, K_{NEC} (see Fig. 8). This basis is a K solution for a semi-elliptical surface crack in an unnotched body, K_{EC} (see Fig. 8), which is given in the literature (**6**). It is assumed that the relative 'difference' between the K value of a semi-elliptical surface crack at a notch and of a semi-elliptical surface crack in an unnotched body is the same as the 'difference' between an embedded circular crack in an infinite body with the notch stress field and the same type of crack within a homogeneous stress distribution, K_{cc}. This leads to the approach presented in Fig. 8.

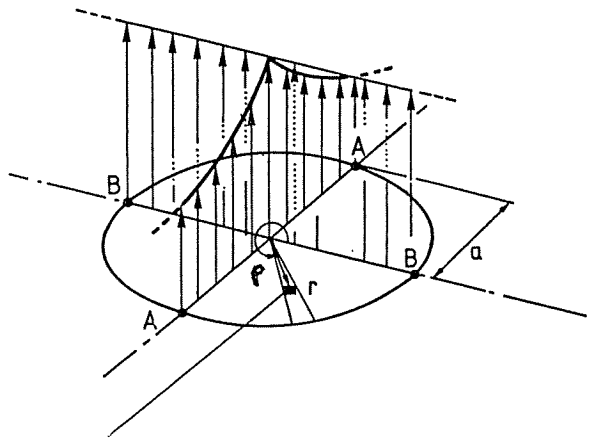

$$P(\varrho,r) = S(\varrho,r) \cdot r d\varrho dr$$

$$P(\varrho,r) = \text{force}$$

$$K_A = \int_0^{2\pi} \int_0^a \frac{S(\varrho,r) \cdot r\sqrt{a^2-r^2}}{\pi\sqrt{\pi a}\,(a^2+r^2-2a \cdot r \cdot \cos(\varrho-\pi/2))} d\varrho \cdot dr$$

$$K_B = \int_0^{2\pi} \int_0^a \frac{S(\varrho,r) \cdot r\sqrt{a^2-r^2}}{\pi\sqrt{\pi a}\,(a^2+r^2-2a \cdot r \cdot \cos\varrho)} d\varrho \cdot dr$$

$K_{A,B}$ = stress intensity factors at A,B

Fig 7 Stress intensity factors at A and B for an embedded three-dimensional crack

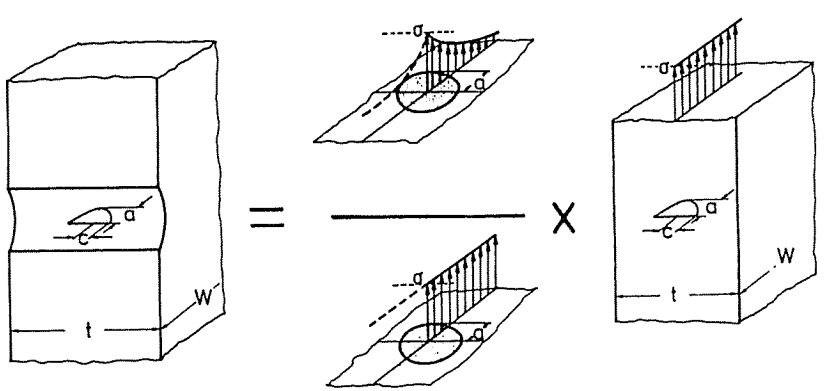

$$K_{NEC} = \frac{K_{NCC}}{K_{CC}} \times K_{EC}$$

K_{NCC} after figure 7

$$K_{CC} = \sigma \cdot \sqrt{\pi a} \cdot \frac{2}{\pi}$$

$$K_{EC} = \sigma \sqrt{\frac{\pi a}{Q}} \cdot F(a/c, a/W, c/t, \Phi)$$

Fig 8 Similarity approach for the stress intensity factor at a notch (three-dimensional case)

Evaluation of the crack growth behaviour

The ΔK solution as proposed in the previous section can immediately be applied to calculate the crack propagation rate on the basis of da/dN vs ΔK data from long cracks as long as no plasticity occurs at the notch tip. If, however, plasticity is present, a correction has to be performed. As shown in Fig. 9 for the notch specimen with $K_t = 3.3$ (for which a finite element calculation had been performed for a nominal loading of the specimen of 100 ± 60 MPa) plasticity occurs during the first uploading of the specimen and a redistribution of the stresses takes place. Afterwards the cyclic stresses behave predominantly elastically (because about twice the yield stress is available for further cyclic

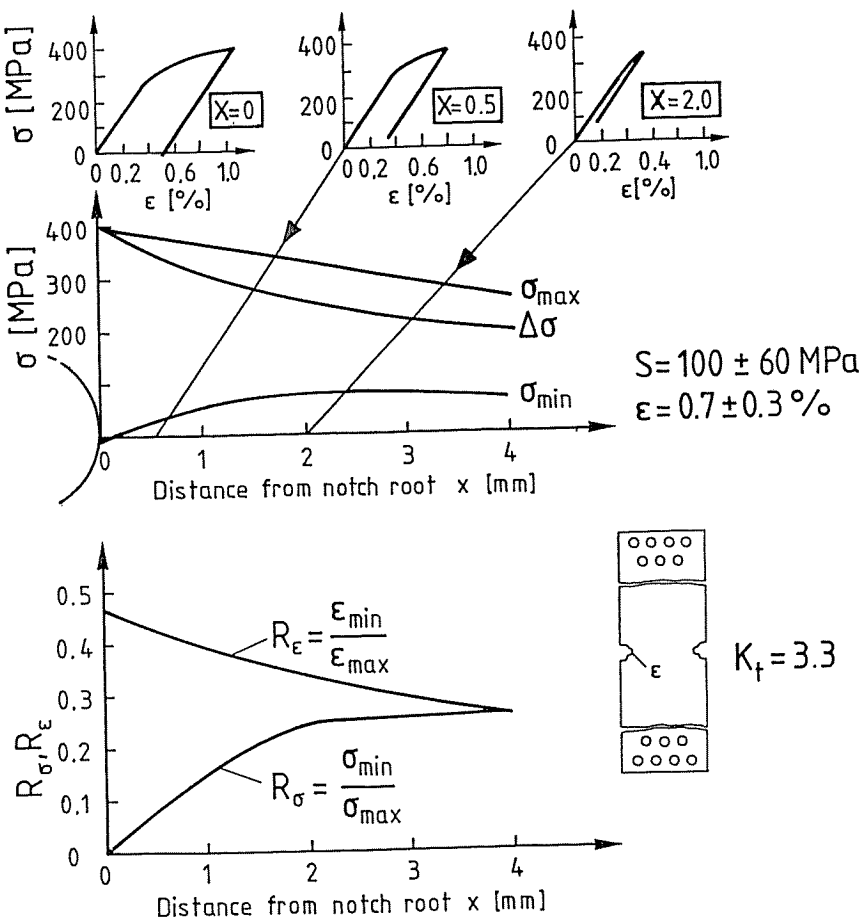

Fig 9 Behaviour of stresses and strains (without a crack) as a function of the distance from the notch for the $K_t = 3.3$ specimen, and behaviour of the stress ratio, R_σ, and the strain ratio, R_ε

loading due to the Masing criterion). This is shown in the insert of Fig. 9 on the left for a distance from the notch root of $x = 0$. At some distance from the notch root the amount of plasticity caused during uploading decreases.

From the local stress–strain paths in the other inserts of Fig. 9 local stress and

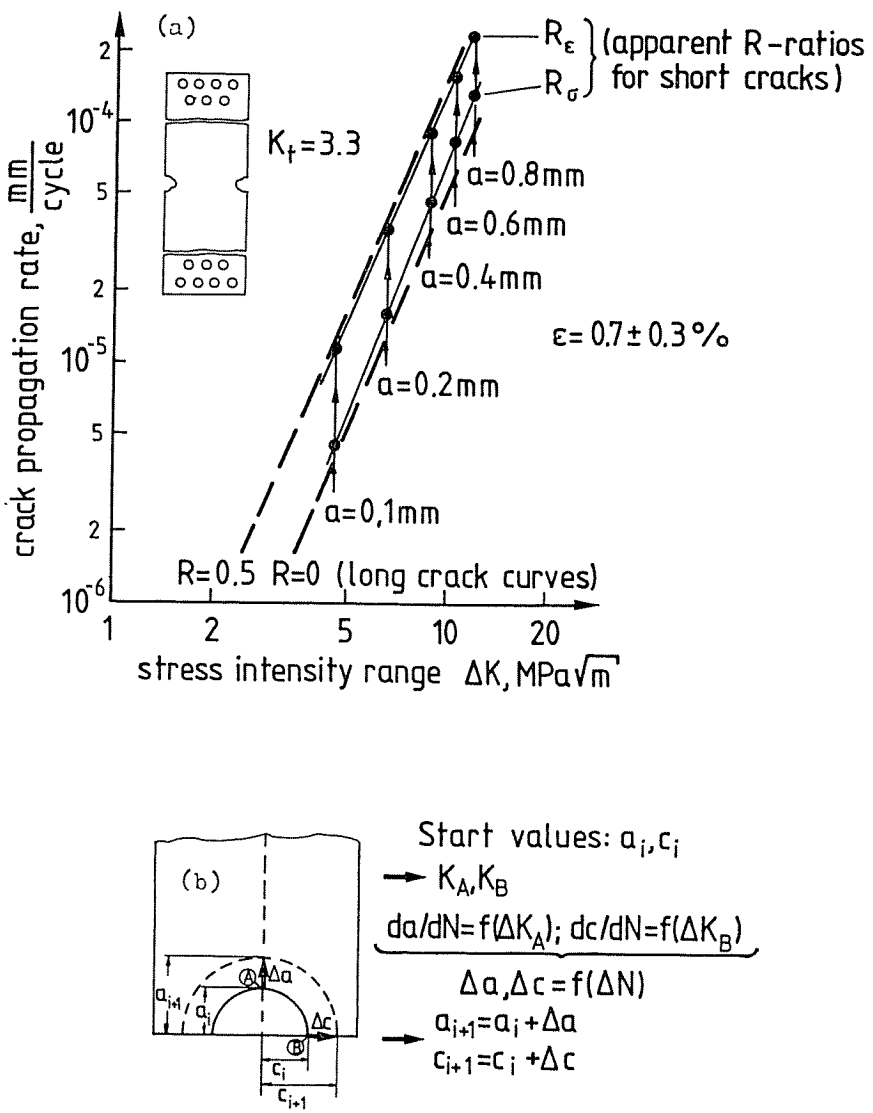

Fig 10 Crack growth prediction on the basis of the apparent R ratios, R_σ and R_ε for short cracks.
(a) Evaluation of apparent R ratios for short cracks
(b) crack growth prediction (schematic)

local strain ratios ($R_\sigma = \sigma_{min}/\sigma_{max}$ and $R_\varepsilon = \varepsilon_{min}/\varepsilon_{max}$, respectively) can always be calculated for cyclic loading. As shown in the lower part of Fig. 9 the parameter R_ε decreases while R_σ increases as the distance from the notch root increases; both R_σ and R_ε approach the nominal stress ratio for very large x values.

It is well established that the crack propagation behaviour of long cracks depends on the R ratio of the nominal stresses. As shown in Fig. 9, local stress and local strain ratios occur which change as a function of the distance from the notch root. It seems reasonable to take the local stress ratio for crack propagation calculations for short cracks at notches. Another possibility is to take the strain ratio, R_ε (**3**)–(**5**). In Fig. 10(a) the apparent R ratios, R_σ and R_ε, are shown on the basic (long crack) da/dN vs ΔK curves. These modified curves are taken as a basis for the consideration of the propagation behaviour of the short cracks. In Fig. 10(b) a crack growth calculation scheme for semi-elliptical surface cracks is outlined. If this procedure is applied (together with the modified data in Fig. 10(a)) to calculate the crack propagation rates for the conditions as were present in the experiments indicated in Fig. 5, the behaviour in Fig. 11(a) can be observed. From the figure it can be seen that neither the R_σ based nor the R_ε based crack propagation calculations represent the experimental short crack behaviour exactly. At shorter crack lengths the R_ε based predictions yield better results. The R_σ based calculations always follow the lower bound of the scatter band of the test data. At longer crack lengths the R_ε based predictions overestimate the actual crack rates. This may be due to the fact that several short cracks may coalesce and form a flat elliptical surface crack. This leads to lower crack propagation rates along the specimen surface as compared to a situation, where the shape of the crack has already reached a stabilized condition.

From an engineering standpoint the more conservative R_ε-based predictions may be preferred. It is also important to note that at very short crack lengths both types of prediction tend to fail. The R_ε approach is essentially similar to the 'strain based stress intensity' concept.

The given trends are further supported by Fig. 11(b), where the experimental results and the crack propagation predictions are compared for the unnotched specimen type of Fig. 2.

So far we have mainly considered mechanically short cracks. In a recent study the behaviour of microstructurally short cracks has been investigated, as well (**13**) and these results are given in Fig. 12. It can be seen that for very short cracks the observed crack propagation behaviour is very different from that of long cracks. But the hatched area, which represents the results from the tests with mechanically short cracks on the specimen types of Fig. 2, deviates from the long crack curve into the zone of lower da/dN vs ΔK values as well.

The present study considers the behaviour of predominantly mechanically short cracks. If Fig. 12 is considered, where the da/dN vs ΔK data of microstructurally short cracks are also shown, a representation of the behaviour seems to be possible if the long crack ΔK threshold value is shifted into the direction of

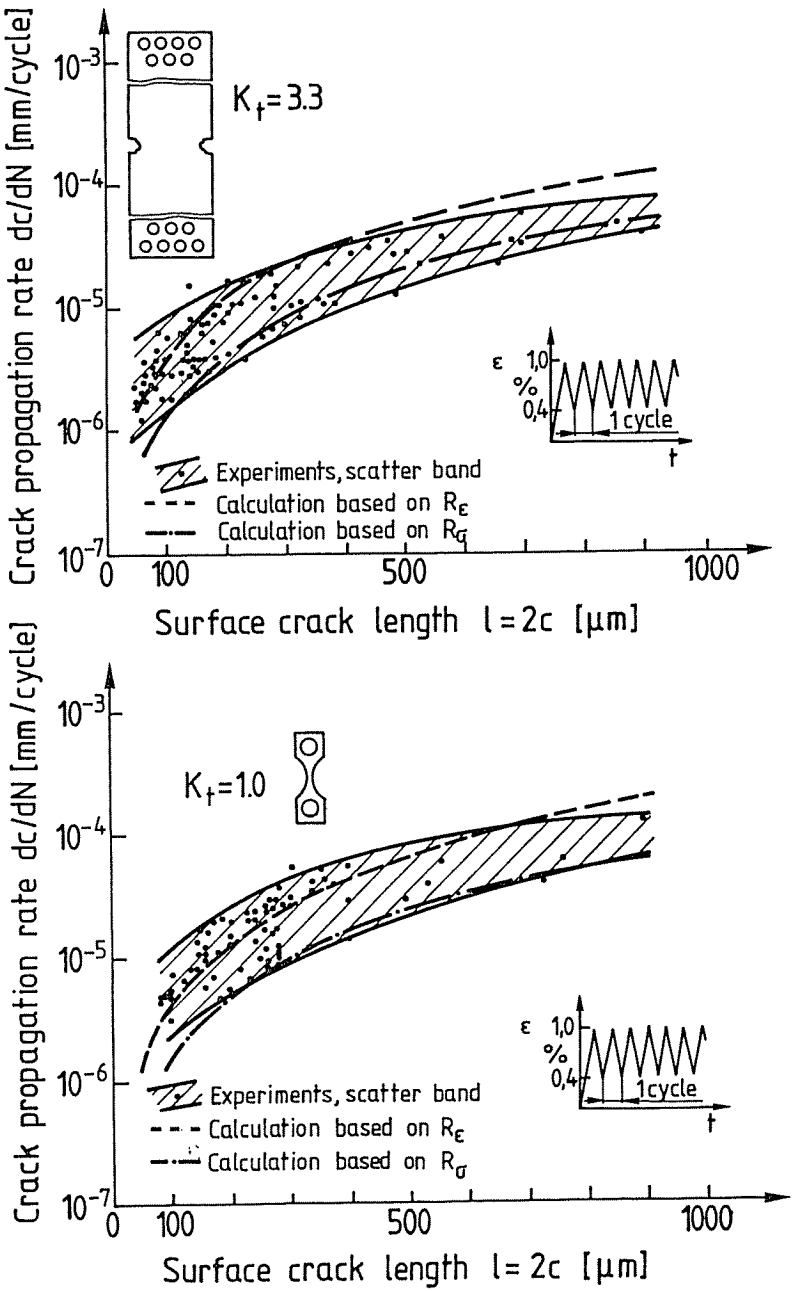

Fig 11 Crack growth calculations based on R_σ and R_ε for the experimental data from Fig. 5 and for the unnotched specimen in Fig. 2

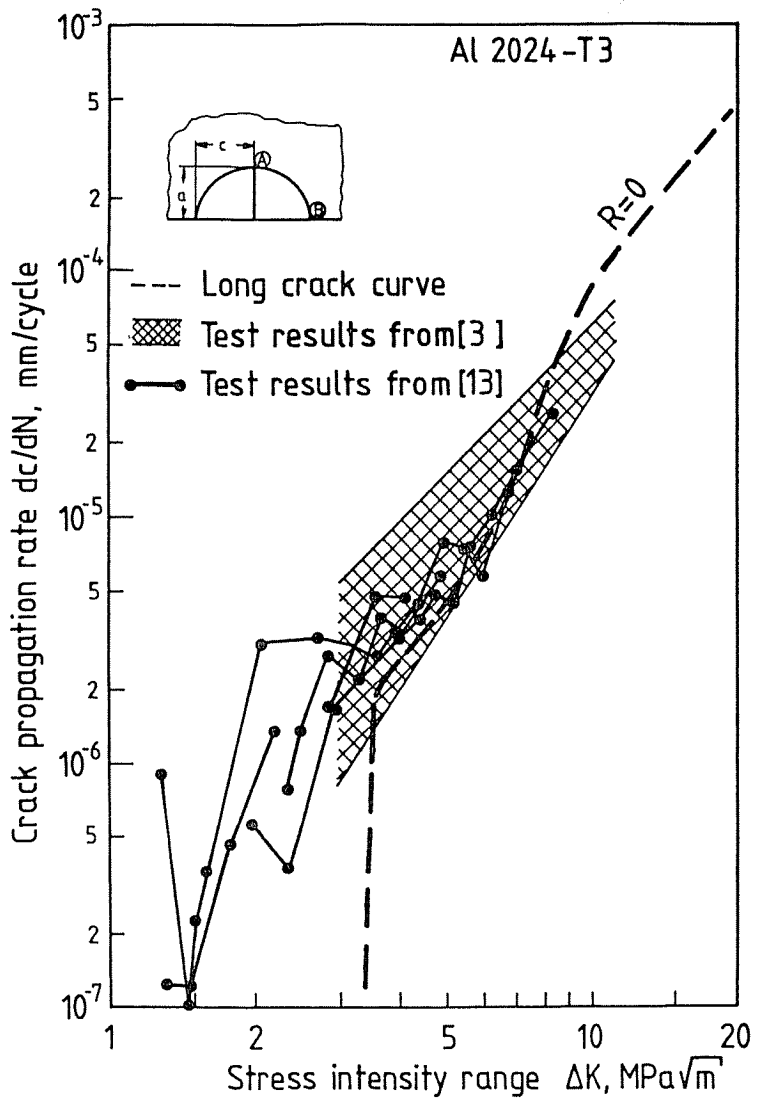

Fig 12 Representation of the behaviour of microstructurally short cracks and of mechanically short cracks in a dc/dN vs ΔK representation

$\Delta K = 0$. Similar trends have also been recognized in references (**14**) and (**15**). In (**1**) a more detailed discussion of the threshold behaviour of short cracks is presented.

Conclusions

On the basis of the results of an extensive experimental program on unnotched and notched Al 2024-T3 specimens a fracture mechanics based evaluation of short crack behaviour was performed. The trends of the observed short crack behaviour are represented in an adequate manner on the basis of a stress intensity concept which incorporated the notch root strain ratio.

Remaining limitations in this concept may be overcome by an investigation into the influence of prior deformation on material behaviour.

Acknowledgements

The support of the Deutsche Forschungsgemeinschaft (DFG) for this investigation is gratefully acknowledged. The authors also thank Mrs Schmidt and Mr Hermanns for their help in preparing the manuscript.

References

(1) NOWACK, H., MARISSEN, R., TRAUTMANN, K. H., and FOTH, J. (1986) Significance of the short crack problem as a function of fatigue life range, *International Conference on Fatigue of Engineering Materials and Structures*, Sheffield 15–19 September 1986.

(2) SCHIJVE, J. (1984) The practical and theoretical significance of small cracks. An Evaluation, *Fatigue 84* (2nd International Conference on Fatigue and Fatigue Thresholds), (EMAS, Warley), pp. 751–772.

(3) FOTH, J. (1984) Einfluß von einstufigen und nicht-einstufigen Schwingbelastungen auf Rißbildung und Mikrorißausbreitung in Al 2024-T3, DFVLR-Rep. No. FB 84-29, DFVLR, D-5000 Cologne 90.

(4) FOTH, J., MARISSEN, R., NOWACK, H., and LÜTJERING, G. (1984) A fracture mechanics based description of the propagation behaviour of small cracks at notches (Edited by L. Faria), *Proceedings of ECF-5*, Lisbon, pp. 135–143.

(5) FOTH, J., MARISSEN, R., NOWACK, H., and LÜTJERING, G. (1984) Fatigue crack initiation and microcrack propagation in notched and unnotched aluminium 2024-T3 specimens, Proceedings of the ICAS Symposium, Toulouse, France, pp. 791–801.

(6) NEWMAN, J. C., Jr., and RAJU, I. S. (1981) An empirical stress intensity factor equation for the surface crack, *Engng Fracture Mech.*, **15**, 185–192.

(7) ROOKE, D. P. and CARTWRIGHT, D. J. (1976) *Compendium of stress intensity factors* (HMSO, London).

(8) TADA, H., PARIS, P. C., and IRWIN, G. R. (1973) The stress analysis of cracks handbook, Del Research Corporation, St. Louis, Missouri.

(9) NEWMAN, J. C., Jr. and RAJU, I. S. (1983) Stress-intensity factor equations for cracks in three-dimensional finite bodies. *Fracture Mechanics: Fourteenth Symposium – Volume I: Theory and Analysis, ASTM STP 791* (Edited by J. C. Lewis and G. Sines), pp. I-238–I-265.

(10) SCHIJVE, J. (1982) The stress intensity factor of small cracks at notches, *Fatigue Engng Mater. Structures*, **5**, 77–90.

(11) JAERGEUS, H. Å. (1978) A simple formula for the stress intensity factors of cracks in side notches, *Int. J. Fracture*, **14**, R113–R114.

(12) OTT, W. (1982) Elastisch-plastische FE-Analyse an Kerben, Ber. Bd. Betriebsfestigkeit von Leichtbauwerkstoffen, DFVLR, D-5000 Cologne 90.

(13) FOTH, J. (1986) AGARD collaborative effort on short cracks, IABG Techn. Rep. TF-V, to be published.
(14) SOCIE, D. F., HUA, C. T., and WORTHEM, D. W. (1985) Mixed mode small crack growth, *Int. J. Fatigue Fracture Engng Mater. Structures*, To be published.
(15) HEITMANN, H. H., VEHOFF, H., and NEUMANN, P. (1984) Life prediction for random load fatigue based on the growth of microcracks, Proceedings 6th International Conference on Fracture (ICF 6), New Delhi, India.